GRAPHENE QUANTUM DOTS WITH ITS AMINO-FUNCTIONALIZATION PREPARED BY MICROWAVE- HYDROTHERMAL METHOD

L. M. DONG[a,b*], K. J. Wu[a], D. Y. SHI[a], X. J. LI[a], Q. LI[a], Z. D. HAN[a,b]
[a]*College of Materials Science and Engineering, Harbin University of Science and Technology, Harbin, China*
[b]*Key Laboratory of Engineering Dielectrics and Its Application, Ministry of Education, Harbin University of Science and Technology, Harbin, China*

N, N-dimethyl formamide was used as the ammonia source, amino-functionalized graphene quantum dots (af-GQDs) were prepared by the microwave–solvothermal method. As confirmed by the structural analysis, the intensity of the af-GQDs (002) crystal plane diffraction peak is greater than GQDs, and the corresponding 2θ diffraction angle is right shift to 25.7°, and the interplanar spacing is reduced to 0.35 nm. Amino-functionalization has significant influence on the crystallization degree and the layer spacing of GQDs, and the size is less than 10 nm, which is closed to zero dimension state. The af-GQDs have strong absorption in the ultraviolet region ($\lambda \leq 276$ nm), but it has no significant characteristic absorption peak, which fits with the semiconductor nanomaterials ultraviolet absorption spectrum. The fluorescence emission spectrum of GQDs were synthesized by this method perform excitation-dependent PL behaviors. The excitation-dependent PL behaviors may be associated with electronic transitions between electronic surface state level and the LUMO energy level.

(Received September 10, 2015; Accepted October 28, 2015)

Keywords: Graphene quantum dots, Microwave, Solvothermal, Fluorescence properties, Amino-functionalized

1. Introduction

In recent years, with the study of graphene materials continuing to rise, graphene quantum dots (GQDs) because of the minisize approximate zero dimensional apparent quantum confinement[1,2] and edge effects[3] has been more attractive application prospect in many areas such as solar photovoltaic devices, biological medicine, light-emitting diodes and sensor, GQDs showing considerably low toxicity, high stability[4], high electrical conductivity and high thermal conductivity. In particular, recent advances have been made in the solution synthesis of colloidal GQDs[5], which provides a solution platform to investigate their optical and optoelectronic properties as well as novel applications, and graphene quantum dots (GQDs) have attracted great attention for their unique properties[6,7]. Because of their great scientific and technological interests, it is of importance to develop their size- and shape-controlled synthetic methods, including top-down[8,9,10]and bottom-up strategies[11,12]. The main methods for preparing graphene quantum dots include hydrothermal

* Corresponding author: donglimin@hrbust.edu.cn

graphene oxide reduction[13,14,15]electrochemical[16] and metal-catalyzed[17]approaches, chemical synthesis[18,19] chemicalexfoliation[20], electron beam lithography[21], and pulsed laser synthesis. Recent years, a microwave pyrolysis method has been developed to prepare carbon nanoparticles[22,23] with particle size ranging from 1 to 5 nm. Microwave-assisted technique has been widely applied to materials synthesis. The GQDs were prepared by a micro-wave-assisted hydrothermal method that combined both the advantages of hydrothermal and microwave techniques[24]. The microwave heating provides rapid, simultaneous, and homogeneous heating, leading to uniform size distribution of quantum dots, thus reaction time is dramatically shortened, product yields and purities was greatly improved[25] . Tang et al. reported a microwave-assisted hydrothermal method that combined both the advantages of hydrothermal and microwave techniques to pyrolyze the glucose.

2. Materials and Methods

2.1. Materials Preparation

The GO nanosheets were synthesized by traditional Hummers method. It was heated by a conventional microwave oven at a certain power (300, 500, 800 and 1000 W) for a period of time (1, 3, 5, 7 and 9 min) to complete the pre-processing of precursor. After cooling to room temperature, the sample was dissolved by N, N dimethylformamide (DMF). After doing ultrasonic treatment for several hours, the mixture was transferred into polytetrafluoroethylene autoclave and heated in different temperatures for a certain amount of time. After completing the reaction, the supernatant was transferred into 1000 Da dialysis tubing, and dialyzed the supernatant by deionized water for many times, then the af-GQDs were obtained. The experimental parameters had a distinct effect on the growth of GQDs such as microwave power, heating time, source concentration, etc.

2.2. Analysis Methods

TEM measurements were performed on JEOL, JEM-2010F at operating voltage of 200 kV. The Fourier transforming infrared (FTIR) spectra of the samples were obtained using the KBr pellet method by Thermo Nicolet Avatar 360 spectrometer with a resolution of 4 cm^{-1}. For PL characterizations, the excitation and emission spectra of the GQDs solutions were recorded by Shimadzu RF-5301PC Analytical Instrument apparatus with Xe lamp as excitation source.

3. Result and Discussion

3.1 Analysis of the structure and morphology of the precursor

We analyze the structure and the morphology of the precursor. Figure 3-1 shows the X-ray diffraction spectrum of the GO before and after experimental treatment. Curve a is the XRD spectrum of the GO that was prepared by the microwave-assisted hydrothermal method, and the curve b is the XRD spectrum of the precursor after secondary oxidation processed. As shown in Figure 1, the two diffraction peaks of GO (001) crystal face are all between 10 ° ~ 15 °. After microwave thermal reduction and secondary oxidation, the diffraction peak of (001) crystal face is from 12.84 ° to 10.25 ° to the left, and the layer spacing is from the initial 0.688 nm increased to

0.862 nm. It means that after the second oxidation, the exfoliation degree of graphite sheet is further improved.

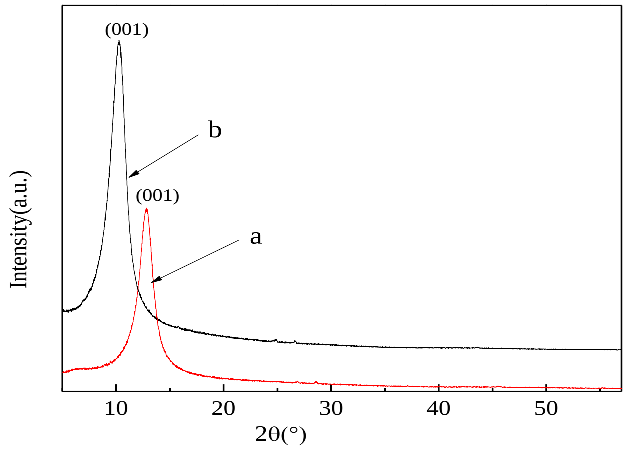

Fig. 3-1 XRD of graphene oxide before and after treatment

a）before treatment　　b）after treatment

Fig. 3-2 shows the TEM spectrum of the GO before and after pretreatment. The figure 3-2 a) shows the GO prepared by the traditional Hummers, and we can find the the exfoliation degree of graphite sheet is not completed, and the thickness of GO is large. The figure 3-2 b) shows the GO prepared by the ultrasonic-assisted Hummers. We can find that the GO prepared looks like transparent film, and part of the GO wrinkles. These results indicate that the oxidation of the graphite sheet is more thoroughly. As shown in figure 3-2 c), the reduction of graphene oxide is obtained after microwave heated reduction. It can be found that agglomeration occurs since the hydrophilic oxygen-containing groups on the surface of the graphene were removed. The stretch degree of graphene is weaker than GO. The figure 3-2 d) is the TEM spectrum of the precursor after secondary oxidation processed, its size was far smaller than the graphene oxide before secondary oxidation processed.

From the Fig. 3-2 we can see that with the improvement of the experimental method, and the layer thickness of graphene oxide changed changed significantly. Graphite was oxidized and exfoliated more thoroughly after ultrasonic-assisted Hummers, and the thinner graphene oxide was obtained. The external energy was added in the graphite oxidation reaction stage, and the ultraphonic provided simultaneous, homogeneous, and fast heating. With the intercalation reactions of oxidants, the vibration frequency of sulfate and metal ions is increased, and that's make them easier to carry out intercalation between the graphite layers. The intercalation agents were hydrolyzed to oxygen-containing group such as -COOH or -CHO during the latter part of the high temperature hydrolysis.

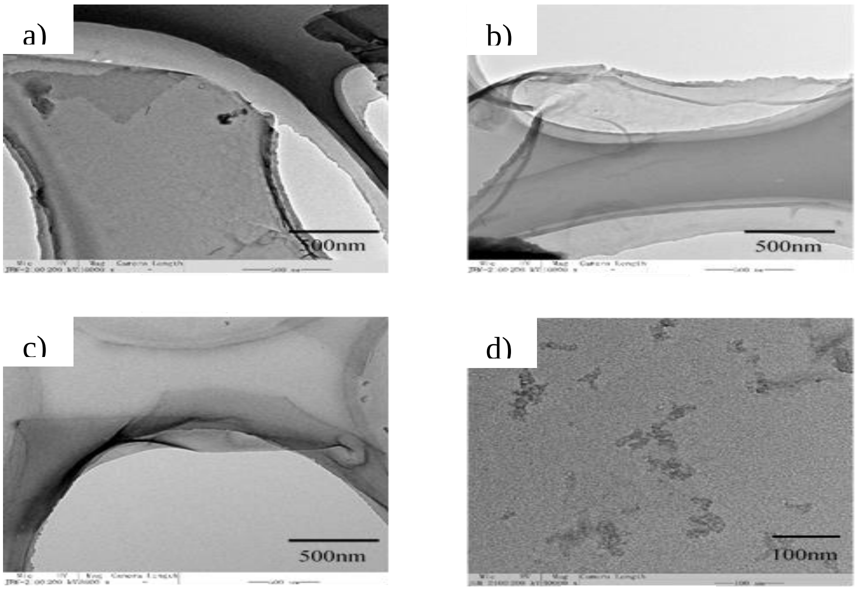

Fig. 3-2 TEM of graphene oxide before and after processing

The reduction of graphene oxide(RGO) is obtained after microwave heated reduction. Compared with the GO, the RGO is nearly transparent, and it means the thickness is further decreased. This is because the microwave treatment provided enough energy to the graphene oxide in a short time, and the unstable oxygen-containing groups between the layers as well as at the edge of the graphite were removed in the form of gases. After the secondary oxide, the size of the graphene oxide decreased significantly. As shown in figure 3-2 d), samples are in the form of fragmented distribution, and the size of the GO is less than 100 nm. The reaction process is in line with unzipping mechanism[26] (Figure 3-3). In the process of acid oxidation, bridging oxygen atom (C-O-C) tend to be arranged in line, and this is easy to disconnect the C-O bond. Once the epoxy bond is opened, it is easy to form a more stable C = O / COOH group at the room temperature. These groups form epoxy chain on graphene nanosheets[27](Figure 3-2). These linear defects make the graphene oxide easily broken.

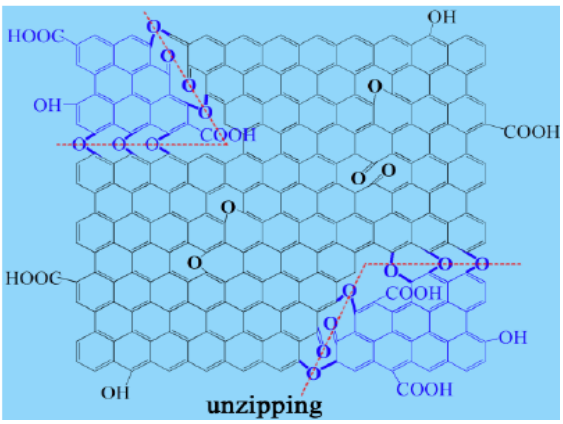

Fig. 3-3 Unzipping mechanism

3.2 The GQDs were prepared by microwave-assisted hydrothermal method

3.2.1 Structure and morphology analysis

Figure 3-4 shows the XRD pattern of the GQDs prepared by different preparation technology. Curve a shows the XRD pattern of GQDs which were prepared by the hydrothermal reaction at 190 ℃ for 10 h; When the GO sheets were under 800 W for 9 min, and then the hydrothermal reaction was carried out at 190 ℃ for 6 h, then we get the XRD pattern of GQDs (curve b). From the Figure 3-4 we can find that the intensity of the GQDs (002) crystal plane diffraction peak increased significantly after doing microwave-assisted hydrothermal method, and the crystallinity is also increased, and this is consistent with the TEM. At the same time the diffraction peak of (002) crystal face is from 27 ° to 24 ° to the left, the interplanar spacing is increased to 0.37 nm. Microwave provides simultaneous, homogeneous, and fast heating in a short time. Since the polarization effect of the microwave reaction reduces the activation energy of the reactants, thereby the rate of reaction is increased.

After microwave processing, hydrothermal reaction time is shortened from 10 h to 6 h. Microwave-assisted hydrothermal method not only makes the structure of the GQDs more complete, but also can be shorten the reaction time significantly.

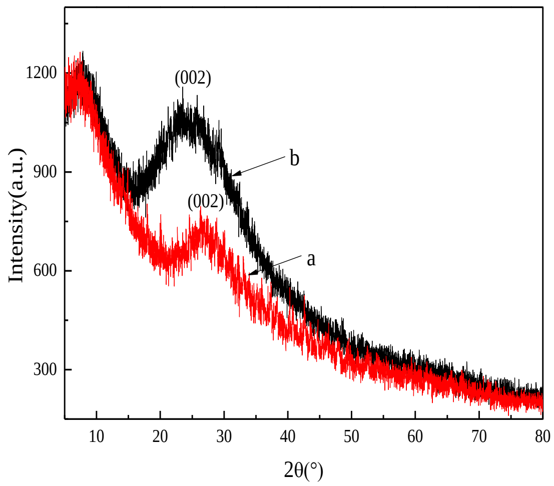

Fig. 3-4 XRD pictures of GQDs prepared by different methods

TEM characterization of the above samples were obtained as shown in Figure 3-5**.** Figure 3-5 a) shows the TEM pattern of GQDs which were prepared by the hydrothermal reaction at 190 ℃ for 10 h; When the GO sheets were prepared by microwave-assisted hydrothermal method, 800 W for 9 min, and then the hydrothermal reaction was carried out at 190 ℃ for 6 h, then we got the TEM pattern of GQDs, as shown in figure 3-5 b). From the Figure 3-5 b) we can find the size of the GQDs is between 7 and 24 nm with microwave assisting, and the average size is about 20 nm. Samples approximate spherical particles, and we can see the lattice fringes. Without microwave processing, the size of the GQDs is about 24 nm, and the lattice fringe is not clear, and the crystallinity is not high. Microwave processing can improve the crystallinity of the sample, and the smaller graphene nanosheets can be got, these facilitates the formation of the GQDs.

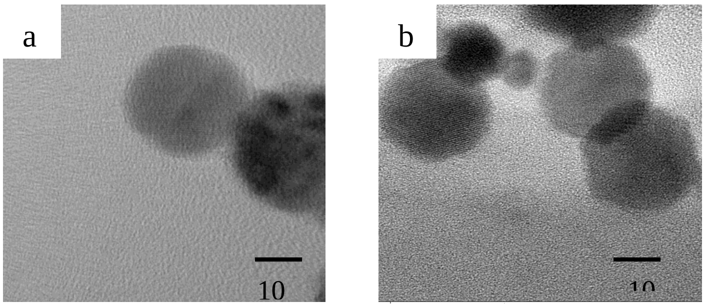

Fig. 3-5 TEM pictures of GQDs prepared by different methods

3.2.2 Functional group analysis

Fig. 3-6 shows the FT-IR pictures of GO and GQDs. As we can see from Figure 3-6, GO has many characteristic absorption peaks, and they are located at 3440 cm^{-1} (V_{-OH} water), 1731 cm^{-1} (Vc = o aldehyde), 1625 cm^{-1} (Vc = o ketone), 1384 cm^{-1} (V_{-CH3}), 1091 cm^{-1} (V_{C-O-C} ethers). Compared with the fourier infrared (FT-IR) spectrum of GQDs, the stretching vibration at 1091 cm^{-1} (C-O-C) disappeared. The C-O-C (aryl ether) stretching vibration peak at 1025 cm^{-1} appears. Hydroxyl stretching vibration peak appears at 1324 cm^{-1}, and the bending vibration peak of the -CH_2 appears at 1448 cm^{-1}, while the stretching vibration peak of aldehyde group at 1729 cm^{-1} disappeared.

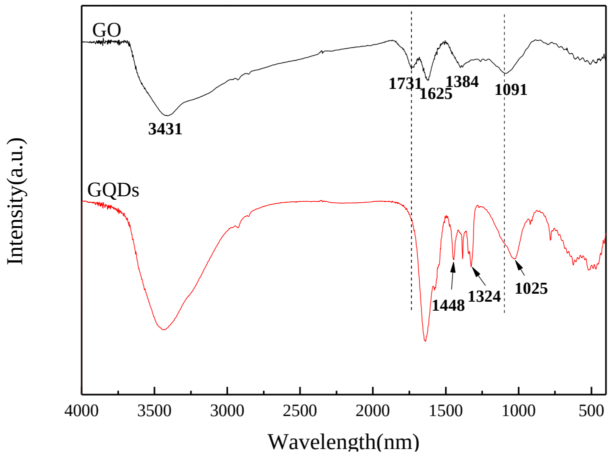

Fig. 3-6 FT-IR pictures of GO and GQDs.

From the figure we can see the disappearance of the aldehyde group, and we take the sodium hydroxide to adjust the pH and introduce the hydroxyl , and the reaction of hydroxyl and hydrogen ions of aldehyde group to produce water, and the -CH_2-CO- is formed. Furans epoxy groups in the carbon-oxygen bonds were broken, and the bridging oxygen atoms were removed, and that's the key to cut the graphene oxide into small-sized graphene quantum dots. During the experiment, hydroxyl functional group introduced by sodium hydroxide has changed the functional groups types of GQDs. The deprotonation process has a great influence on the fluorescence properties of the GQDs.

3.3.3 Analysis of Fluorescence Properties

Figure 3-7 shows the normalized fluorescence spectrum and ultraviolet visible absorption spectrum. GQDs maximum excitation wavelength is 314 nm, corresponding emission wavelength is 430 nm, and the stokes shift is 116 nm. We can get the CIE coordinates through the emission peak datas, GQDs releases blue fluorescence by the chromaticity diagram analysis. GQDs have two excitation peaks located at 257 nm and 314 nm, and its fluorescence emission peaks are all located at 430 nm, and the emission band is due to the $\sigma \rightarrow \pi^*$ and $\pi \rightarrow \pi^*$ transition. UV absorption spectrum shows that GQDs have absorption in the ultraviolet region, which is due to the $\sigma \rightarrow \pi^*$ transition of sp^2 aromatic group.

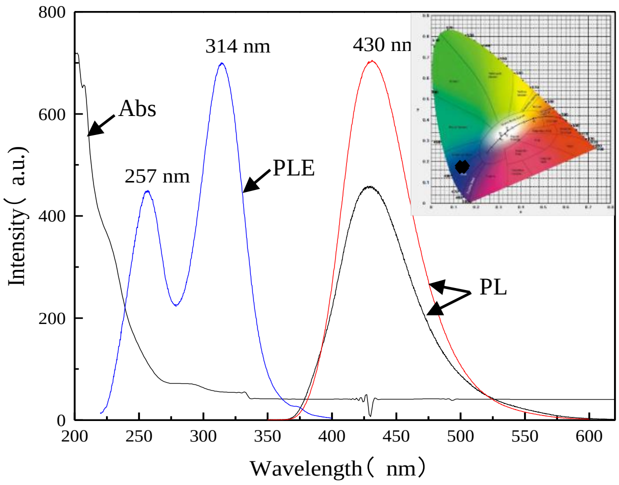

Fig. 3-7 Normalized fluorescence spectrum and ultraviolet visible absorption spectrum of GQDs prepared by microwave-assisted hydrothermal method

The fluorescence properties of GQDs are related to the carbene structure of triplet electron transition. For triplet $\sigma^1\pi^1$ structure, σ and π-orbital were occupied by unpaired electrons. In the process of triplet electron transition, the electrons from the σ and π orbital track (Highest occupied molecular orbital, HOMO) jump into the π* orbital (Lowest unoccupied molecular orbital, LUMO). In GQDs emission process, electrons from π orbital jump into the LUMO energy levels, and the required energy is 4.15 eV (314 nm). Electrons from the σ orbital jump into the LUMO energy levels, and the required energy is 5.07 eV (257 nm). As shown in Figure 3-8, the energy gap (δE) between the σ and π is 0.92 eV, and the value is consistent with the triplet carbene theoretical value δE (<1.5 eV) [28]. Therefore, when the energy reaches the required energy for electron transitions from σ and π orbital to the LUMO, and electron transitions will occur; fluorescence is generated when the energy changed from the LUMO to the lower energy state.

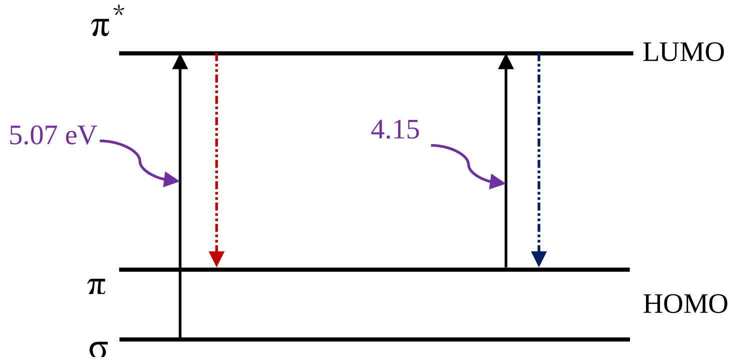

.*Fig. 3-8 Electron transition diagram of GQDs striplet state*

3.3 GQDs amino functional analysis

3.3.1 af-GQDs structure and morphology analysis

N, N- dimethyl formamide was used as the ammonia source and solvent, amino-functionalized graphene quantum dots (af-GQDs) were prepared by the microwave – solvothermal method.

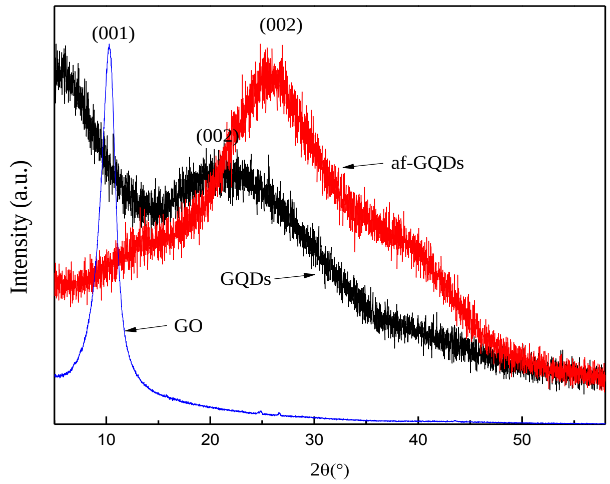

Fig. 3-9 XRD figure of the precursor, GQDs and af-GQDs

Fig. 3-9 shows the XRD pattern of the precursor, GQDs and af-GQDs. (002) crystal face diffraction peak of the af-GQDs was located at 25.7°. The diffraction peak of GQDs (002) crystal face was at 24°, the peak shape looks like bread peak, and the peak is not obvious. The diffraction peak of GO (001) crystal face is about located at 10°, that's a strong and sharp peak. The figure shows that the intensity of the af-GQDs (002) crystal plane diffraction peak is greater than GQDs, the corresponding 2θ diffraction angle is right shift to 25.7 °, and the interplanar spacing is reduced to 0.35 nm. Amino-functionalization has significant influence on the crystallization degree and the layer spacing of GQDs. We analyze that when the nitrogen source reacted with oxygen-containing functional groups in the graphene sheet, and it is easier reacted with the functional groups on the edge. Unreacted oxygen-containing functional groups and bridging oxygen atom are transformed into water or gas etc., and they are removed under the high temperature and high pressure atmosphere. This makes the graphene defects decreased, the graphene crystal structure tends to complete. GQDs interplanar spacing(0.35 nm) is less than the graphene oxide (002) interplanar spacing (0.431 nm), because the oxygen-containing groups between the graphite layers are removed during the reaction at high temperature and pressure.

Figure 3-10 shows the TEM pictures of af-GQDs. Figure 3-11 a) is an enlarged 10,000 times TEM image of the af-GQDs, and the 3-11 b）is an enlarged 60,000 times TEM image of the af-GQDs. The af-GQDs dispersed uniformly without agglomeration. From the high-resolution electron microscope photograph(HRTEM) we can see that the size of the prepared graphene quantum dots is about 5-7 nm, it is closed to the zero-dimensional state. The (002) crystal face lattice fringes of the graphene quantum dots is legible, and the interplanar spacing is about 0.35 nm.

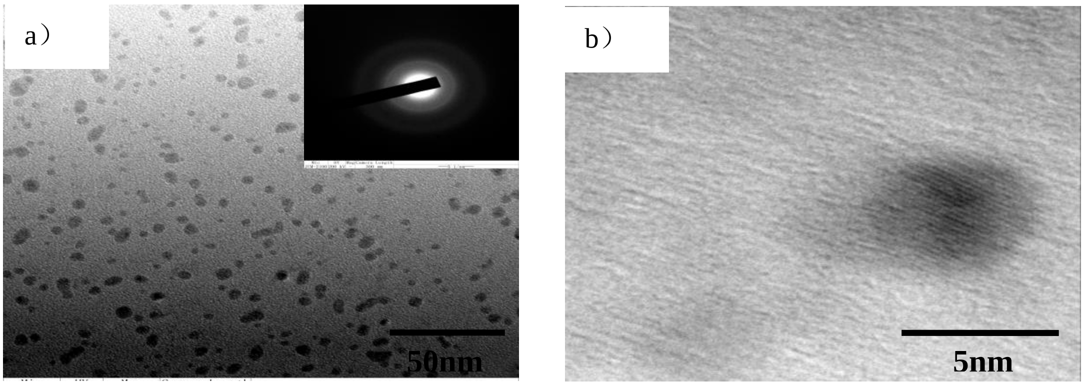

Fig. 3-10 TEM pictures of af-GQDs

3.3.2 Functional group analysis

Fig. 3-11 shows the FT-IR figure of GQDs and af-GQDs. After amino functional modification, the types of af-GQDs functional groups increased significantly. The stretching vibration of CH_2 appears at 2925 cm^{-1}, the absorption band of the sp^2 hybridized carbon ring (benzene nucleus for short) appears at 1448 cm^{-1}. It means that the GQDs structural defects are decreased after microwave-assisted hydrothermal, crystal structure tends to complete. In addition, the hydroxyl weakened and disappeared with the microwave-solvothermal reaction, the number of oxygen-containing groups is also reduced. After a series of reaction, the NH_2 and C-N bending or stretching vibration peaks appear at 2362, 1492, 1263 and 698 cm^{-1}. It means that nitrogen-containing functional groups were introduced.

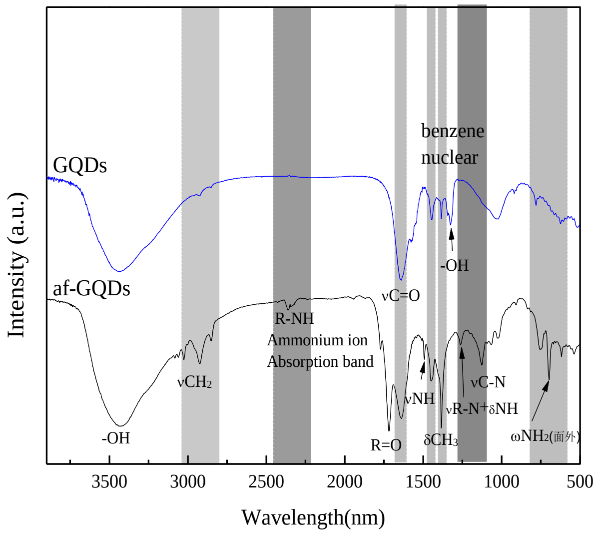

Fig. 3-11 FT-IR figure of GQDs and af-GQDs

3.3.3 Fluorescence Performance Analysis

AF-GQDs have a wealth of fluorescence emission performance. Fig. 3-12 shows the UV-Vis absorption and fluorescence spectra of af-GQDs. The af-GQDs have strong absorption in the ultraviolet region (λ≤276 nm), but it has no significant characteristic absorption peak, which fits with the semiconductor nanomaterials ultraviolet absorption spectrum. In addition, a shoulder peak at 276 nm indicates the existence of functional groups with lone pair electrons (such as carboxyl etc.). In addition, af-GQDs absorbance is decreased at 494 nm, while the maximum emission wavelength ia located at 494 nm.

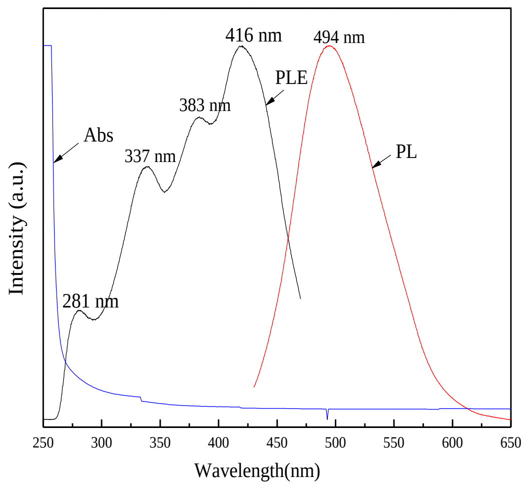

Fig. 3-12 Ultraviolet UV-Vis absorption and fluorescence spectra of af-GQDs

After amino functional modification, the PL spectra of af-GQDs changed significantly. We find the maximum excitation and emission peak redshift 494 nm and 416 nm respectively(416 nm excitation), and the stokes shift is 78 nm. The emission wavelength data was imported CIE color coordinates and calculated, its color coordinate is located in green light-emitting region. Emission wavelength redshift which indicates the energy of the electronic transitions is decreased. After amino functional modification, the electronic structure of graphene quantum dots changed, the band gap between the HOMO and the LUMO was shortened. We analyze that amino groups were introduced into the GQDs edge. With reacting with amino group electron orbit, graphene molecule delocalized π electrons HOMO orbital is moved to the higher energy orbits, and the band gap is shortened consequently.

af-GQDs excitation spectra have four excitation peaks, and they are located at 281, 337, 383 and 416 nm respectively. Figure 3-13 shows the emission spectra of af-GQDs excited by different excitation wavelengths. Although the excitation wavelength changes, the corresponding af-GQDs emission peak wavelength does not change. The maximum emission peak wavelength is about 490 nm. The research shows that with the increasing of the intensity of each excitation peak, the intensity of emission peaks is also increased. When excited by the 416 nm, the highest emission peak intensity is obtained. GQDs have an emission characteristic of multi-wavelength excitation, we analyze that apart from the $\sigma \rightarrow \pi^*$ and $\pi \rightarrow \pi^*$ electronic transition of GQDs carbene structure itself, since the introduction of the nitrogen-containing functional groups, the electron distribution of the af-GQDs surface is changed.

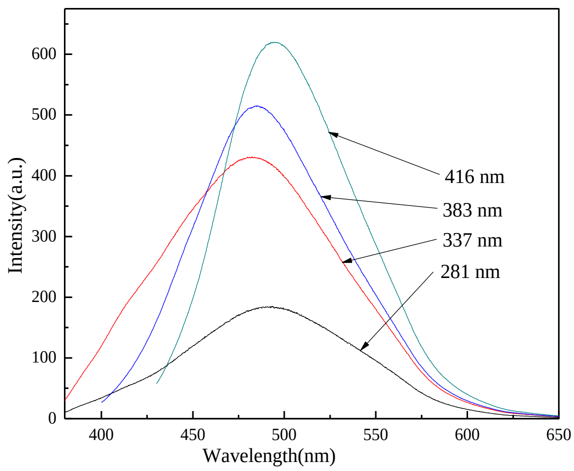

Fig. 3-13 Emission spectra of af-GQDs excited by different excitation wavelengths

To study the relationship between the emission spectrum and excitation wavelength, the af-GQDs were tested by the different excitation wavelengths. Figure 3-14 shows the emission spectra of af-GQDs which were excited by different wavelengths. The inset at the right shows the af-GQDs emitting light colors which were excited by the 420,440,460,480 and 500 nm respectively. With the excitation wavelength changed from 420 nm to 500 nm, the GQDs emission peak wavelength from 497 nm red shift to 546 nm, and the emission intensity is followed by decline. The fluorescence emission spectrum of GQDs that synthesized by this method performs excitation-dependent PL behaviors. The excitation-dependent PL behaviors may be associated with electronic transitions between electronic surface state level and the LUMO energy level.

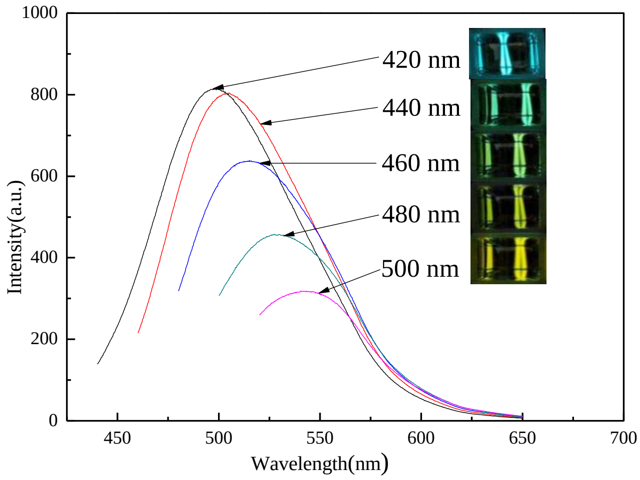

Fig. 3-14 Emission spectra of af-GQDs which were excitated by different wavelengths

4. Conclusion

Highly luminescence GQDs are prepared by a microwave-assisted hydrothermal method. N, N- dimethyl formamide was used as the ammonia source and solvent, amino-functionalized graphene quantum dots (af-GQDs) were prepared by the microwave–solvothermal method. The af-GQDs dispersed uniformly without agglomeration. From the high-resolution electron microscope photograph we can see that the size of the prepared graphene quantum dots is about 5-7 nm, it is closed to the zero-dimensional state. The (002) crystal face lattice fringes of the graphene quantum dots is legible, and the interplanar spacing is about 0.35 nm. With the excitation wavelength changed from 420 nm to 500 nm, the GQDs emission peak wavelength from 497 nm red shift to 546 nm, and the emission intensity is followed by decline. The fluorescence emission spectrum of GQDs that synthesized by this method performs excitation-dependent PL behaviors. The excitation-dependent PL behaviors may be associated with electronic transitions between electronic surface state level and the LUMO energy level. The discovery of the new PL from GQDs may expand the application of graphene-based materials to other fields such as optoelectronics and biological labeling.

Acknowledgment

This work was financially supported by program for innovative research team in university of Heilongjiang province (2013TD008).

References

[1] L A Ponomarenko, F Schedin, M I Katsnelson, et al., Science, **320(**5874), 356 (2008).
[2] L Li, X Yan, The Journal of Physical Chemistry Letters, **1**(17), 2572 (2010).
[3] S Zhu, J Zhang, C Qiao, et al., Chem. Commun, **47**(24), 6858 (2011).

[4] S Liu, X Liu, Z Li, et al., New Journal of Chemistry, **35**(2), 369 (2011).
[5] D Pan, L Guo, J Zhang, et al., Journal of Materials Chemistry, **22**(8), 3314 (2012).
[6] H Jia, X Su, G Hou, CIESC Journal , **64(**5), 1862 (2013).
[7] H He, X Wang, L Bai, Q Guo, CIESC Journal, **65**(6), 2186 (2014).
[8] Y Li, Y Zhao, H Cheng, et al., Journal of the American Chemical Society, **134(**1), 15 (2011).
[9] V Gupta, N Chaudhary, R Srivastava, et al., Journal of the American Chemical Society, **133(**26), 9960 (2011).
[10] J Shen, Y Zhu, C Chen, et al., Chem Commun, **47(**9), 2580 (2011).
[11] J Zhu, J Li, "Quantum Dots," Quantum Dots for DNA Biosensing, Springer Berlin Heidelberg, pp. 9-24, (2013).
[12] R Liu, D Wu, X Feng, et al., Journal of the American Chemical Society, **133**(39), 15221 (2011).
[13] D Pan, J Zhang, Z Li, M Wu, Advanced Materials, **22**(6), 734 (2010).
[14] D Pan, L Guo, J Zhang, C Xi, Q Xue, H Huang, et al., Journal of Materials Chemistry, **22**, 3314 (2012).
[15] J Lu, P S E Yeo, C K Gan, et al., Nature nanotechnology, **6(**4), 247 (2011).
[16] Y Li, Y Hu, Y Zhao, et al., Journal of the Advanced Materials, **23**(6), 776 (2011).
[17] X Yan, X Cui, L Li, Journal of the American Chemical Society, **132**(17), 5944 (2010).
[18] X Yan, X Cui, B Li, et al., Nano Letts, **10**(5), 1869 (2010).
[19] J Peng, W Gao, Z Li, et al., Nano Letts, **12**(2), 844 (2012).
[20] S Schnez, F Molitar, C Stampfer, et al., Applied Physics Letters, **94**, no. 1, (2009).
[21] H Zhu, X Wang, Y LI, Z Wang, F Yang, X Yang, Chem. Commun, no. 34, 5118 (2009).
[22] X Wang, K Qu, B Xu, J Ren, X Qu, Journal of Materials Chemistry, **21**(8), 2445 (2011).
[23] L Tang, R Ji, et al., ACS Nano, **6**(6), 5102 (2012).
[24] E A Anumol, P Kundu P, A Deshpande, et al., ACS Nano, **5**(10), 8049 (2011).
[25] C L Sun, C T Chang, H H Lee, J Zhou, et al., ACS Nano, **5**(10), 7788 (2011).
[26] D V Kosynkin, A L Higginbotham, A Sinitskii, et al. Longitudinal Unzipping of Carbon Nanotubes to Form Graphene Nanoribbons[J]. Nature, **458,** 872 (2009)
[27] Z Li, W Zhang, Y Luo, et al. How Graphene Is Cut upon Oxidation[J]. Am. Chem. Soc., **131,** 6320 (2009).
[28] D Bourissou, O Guerret, F P Gabba, et al. Stable Carbenes[J]. Chem. Rev., **100**, 39 (2000)

.